AALBORG UNIVERSITY
STUDENT REPORT

Damping of Edgewise Vibrations of Wind Turbine Blades by Smart Liquid Dampers

René Bundgaard Andreasen

M.Sc. in Structural and Civil Engineering

Master thesis

June 8th 2017

AALBORG UNIVERSITY
STUDENT REPORT

The School of Engineering and Science
Study Board of Civil Engineering
Thomas Manns Vej 23, 9220 Aalborg Ø
http://www.ses.aau.dk/

Title:

Damping of Edgewise Vibrations of Wind Turbine Blades by Smart Liquid Dampers.

Project period

February 2017 - June 2017

Participant

René B. Andreasen

Supervisor

Søren R. K. Nielsen

Report pages: 37
Appendix pages: 0
Completed June 8th 2017

Synopsis:

This project contains analyses of two different methods of implementation of semi-active control damping to reduce edgewise tip displacement of a wind turbine wing. This is investigated through a feed-back control for an orifice control and with the use of smart fluids to see if it further reduce the tip displacement in comparison to a passive orifice controlled damper. The focus is mainly on the use of the semi-active control of the two different methods which is investigated in a reduced two degree of freedom model for a wind turbine blade. It is found that the semi-active control can achieve similar results in reduction of the edgewise tip displacement, but allows for adaptation when the rotor changes velocity in cut-in, cut-out and when the blade is being pitched. A short discussion on the practical implications for installation of either the orifice control or smart fluid control is presented as well.

Abstract

I dette projekt vil der undersøges metoder til forhindring af kantvise svingninger for vindmøllevinger. Til dette vil der anvendes en numerisk model for en vindmøllevinge der indeholder to frihedsgrader. Modellen indeholder som udgangspunkt et passivt kontrol system af en åbning der accelererer / deaccelererer væsken der er inde i torussen.
Der implementeres et semi-aktivt system der skal anvendes til at kontroller åbningen, samt brugen af smartvæsker, til at udnytte muligheden for et intelligente design, således væsken kan ændres for altid at virke optimalt uanset situation. Der er blevet undersøgt lidt omkring smartvæsker og hvordan de bruges på nuværende tidspunkt for at finde ud af hvordan disse kan implementeres i en vindmøllevinge. Der er taget udgangspunkt i magnetisk væske, hvortil der skal bruges et magnetfelt for at "aktiver" væskens effekt, til at ændre egenskaberne.
Der er blevet udledt modeller for feed-back kontrol som undersøges ved hjælp af to frihedsgradsmodellen hvor resultaterne viser at den semi-aktive kontrollov for en specifik rotationshastighed, ikke forbedre situationen fra den passive kontrol markant, hvilke betyder for den ene hastighed vil det ikke give et bedre resultat for kontrol af åbningen. For smartvæsken var det samme udgangspunkt resultatet havde, det var ikke en markant bedre løsning, men et alternativ der kan anvendes, men der skal ligges vægt på at det er ved en fast rotationshastighed.
Ved brug af semi-aktiv kontrol, skal der være en udefra påvirkning der ændre systemet, men for at udnytte den adaptive effekt ved semi-aktiv kontrol, kan ændringer i rotor hastighed give konsekvenser for centrifugalstivheden når hastigheden af rotoren falder eller stiger, hvilket giver konsekvenser for dæmpningen i systemet.
Derfor undersøges der for smartvæsken og åbningen, hvilke ændringer der bør fortages for at opretholde det optimale dæmpningsforhold for at sikre den mindste mulig vibrationer forekommer. Ved at gøre dette viser resultaterne at den passive model med sammen dæmpningskoefficienter ikke er den optimale længere, og derfor muliggøre den semi-aktive kontrol som den bedre løsning ved at skifte den viskose karakteristik af væsken til den nødvendige situation, som kunne være opstart eller vindmølle vingerne bliver pitchede.
Praktisk kan smartvæskekontrollen være relativt svært at implementer, eftersom det at skabe et magnetfelt omkring væskebeholderen kan gøres med en spole der sættes strøm igennem, men der skal stadig være plads til det, samt smartvæsken er tre gange så tung som vand, hvilket kan give implikationer, når dæmperen gerne skal langt ud i vindmøllevingen og sidde for at optage vibrationerne i spidsen af vingen.

Åbningskontrollen kan være svær at få til at virke optimalt, da responstiden for åbningen kan være svær at få til at være hurtig nok eftersom ændringer i systemet kan ske øjeblikkeligt hvilket kræver responstiden for systemet også skal være øjeblikkeligt, hvilket kan give plads problemer med udstyr/installationer for at kunne opnå tilfredsstillende resultater.

Preface

This report is a master thesis which is the last part of the Master's programme in Structural and Civil Engineering at Aalborg University.

Prerequisites for reading the report is knowledge regarding the wind turbine mechanics, structural mechanics and dynamics.

Gratitude is addressed to the supervisors of the project, prof. Søren R. K. Nielsen for constructive criticism and inspiring supervision during the project.

Front page picture courtesy of Dong Energy A/S.

Reading guide

References to sources are in the form of the Harvard method, and a complete source list is stated in the bibliography. References are made to sources with either "[Surname/organisation, Year]" or "Surname/organisation [Year]" and, when relevant, specific pages, tables or figures may be stated. Websites are specified by author, title, URL and date. Books are specified by author, title, publisher and edition, where available. Papers are furthermore specified with journal, conference papers with time and venue, when available.

The report contains figures and tables, which are enumerated according to the respective chapter. E.g. the first figure in Chapter 3 has number 3.1, the second number 3.2 and so on.

René Bundgaard Andreasen

Table of contents

Introduction 1

In this chapter an introduction is given to the project and a state of the art on the subject.

To meet the increase in demand of more green energy world wide, wind turbines are an excellent option as they can be placed both on land and offshore. Offshore solutions are increasingly chosen because they do not require the same amount of logistics for transportation for multi megawatt machines. Further the environment around onshore wind turbine can cause turbulent inflow, due to of vegetation as trees or tall structures. The negatives for the offshore wind turbines is the cost of the foundation of the wind turbine and in case of damage, the downtime for repairs is considerably longer. The wind turbine is subjected to wind forces, which changes direction and magnitude because of turbulence, which causes a dynamic response of the total structure or substructures of the wind turbine. In this project the focus is on the dynamic response of a wind turbine wing, specific the edge wise vibrations of the wind turbine wing, as illustrated in figure 1.1.

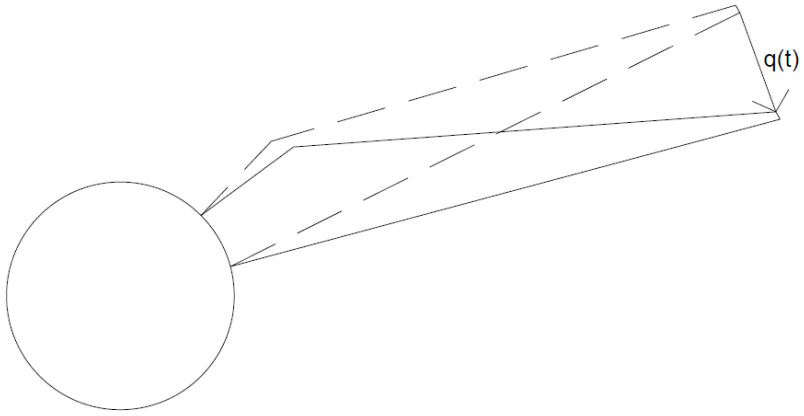

Figure 1.1. Edgewise vibration from the displacement $q(t)$.

This is an issue because in the edgewise vibration are related with little to no aerodynamic damping, so only structural damping is present, which is very small. Some research has already been done on the subject. [Basu et al., 2015] has analysed the problem based on passive control with a circular liquid damper, which has many similarities to this project. The difference is, that in this project is a semi-active control of the liquid damper is applied, either based on a feed-back

control of the orifice opening or based on smart fluid control. These methods will be compared to a passive orifice control to analyse the possible benefits. A more detailed description of smart liquids is given in Chapter 3. The essence of it is that the viscosity of the fluid is controlled via a magnetic or electric field, which provides a mean for feed-back control of the vibrations. The restoring force of the oscillating mass of the damper is caused by the centrifugal force during rotations, which depends on the rotational speed of the rotor. Hence a passive controlled damper will only be optimal tuned at a certain rotational speed. In contrast semi-active controlled dampers can be tuned to a variety of rotational speeds. Smart liquids is not a very well known concept, but it is already in use for suspension systems to cars. Experiments has been preformed to test how the liquid works and its performance as a damping liquid which also can be seen in [Goncalves, 2005].

The semi-active control will be applied to a highly reduced 2-DOF model specifying the edgewise motion of the wind turbine blade and the motion of the fluid in the damper. The use of magneto-rheological fluid as a damping liquid to reduce vibration in general is not new, [J.Y. Wang, 2005] and [J.Y. Wang, 2004]. Their research is done on a tuned liquid damper with the magneto-rheological fluid. The damper was implemented in a tall building susceptible to excitation from wind and/or earthquakes. By controlling the viscosity of the liquid will de-accelerate relative to the frame of the damper which causes a inertia force. The inertia force working upon the secondary system which is then transferred to the primary system which is to counter act the excitation [J.Y. Wang, 2005]. From their research they concluded that using a tuned liquid damper with MR-liquids can achieve better vibration mitigation, than with the conventional methods with the normal tuned liquid damper.

For the use of semi-active control a state-of-the-art review has been made by [Michael D. Symans, 1997], and [N.R. Fisco, 2011] also introduces the magnetorheological fluid dampers. From their research, the combination of using smart materials into a semi-active control of structures should be a more practical approach when passive control of structures is not sufficient enough.

From the indicated review it seems plausible to apply the same ideas for other structures, which can have problems with vibration mitigation, as in examined in this project a wind turbine wing.

Wind turbine mechanics 2

In this chapter the general wind turbine blade damper used in the project will be showed.
The majority of the theory described in this chapter has been derived by B. Basu, Z. Zhang and S.R.K Nielsen from the article [Basu et al., 2015].

2.1 Definition of the problem

Figure 2.1 shows an illustration of a wind turbine blade rotating with the liquid damper implemented. Three different coordinate systems is defined; (X_1, X_2, X_3) is a global fixed coordinate system which has its origin at the center of the hub in the referential state. X_1 is in the direction of the mean wind and the X_3-axis is in the vertical direction. Coordinate system (x_1, x_2, x_3) is fixed to the rigid body part of the motion of the wind turbine wing with center in the hub and x_3 goes along the wind turbine wing. The last coordinate system (y_1, y_2, y_3) is fixed to the frame of the damper with origin in the damper center. The y_1-axis coincides with x_1- and X_1-axis for the damper. in case of no elastic deformation of the blade takes place y_3 and x_3 are coinciding. Coordinate axes (X_1, x_1, y_1) are all uni-directional to the wind direction. The y_3-axis coincides with the x_3 in case of no elastic deformation of the blade. The angle between the x_3- and y_3-axis is denoted φ with the sign definition given in figure 2.1.
The edgewise vibration of the wind turbine blade is described by the coordinate system (x_1, x_2, x_3), while the movement which the liquid do is described in the local coordinate system (y_1, y_2, y_3). The mass per unite length of the blade is denoted $\mu(x_3)$, where the bending stiffness in the edgewise direction is denoted $EI(x_3)$. The edgewise displacement of the blade undergoing vibration is modelled by a single degree of freedom, which is chosen as the edgewise tip displacement $q(t)$ with the sign definition from figure 2.1. The position of the damper in the wind turbine blade is described by $x_0 = 45\,\text{m}$.

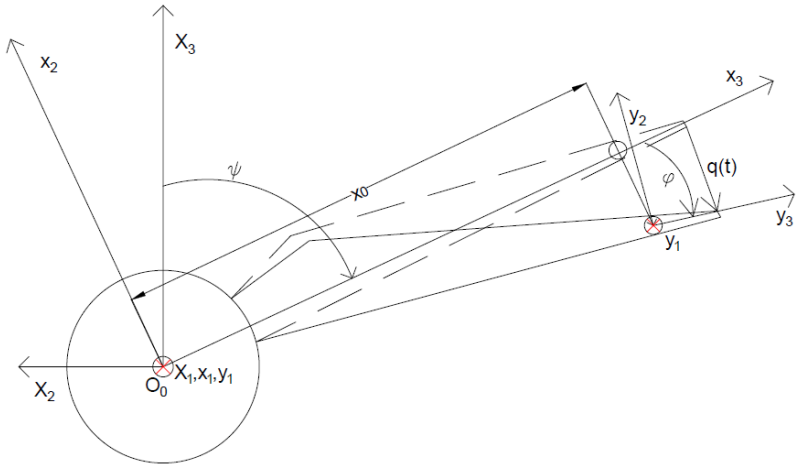

Figure 2.1. Definition of the used coordinate systems, with geometry and DOF. The red cross indicates the axis X_1, x_1, y_1 respectively.

2.2 Damper

A sketch of the damper can be seen in figure 2.2, which has the shape of a torus.

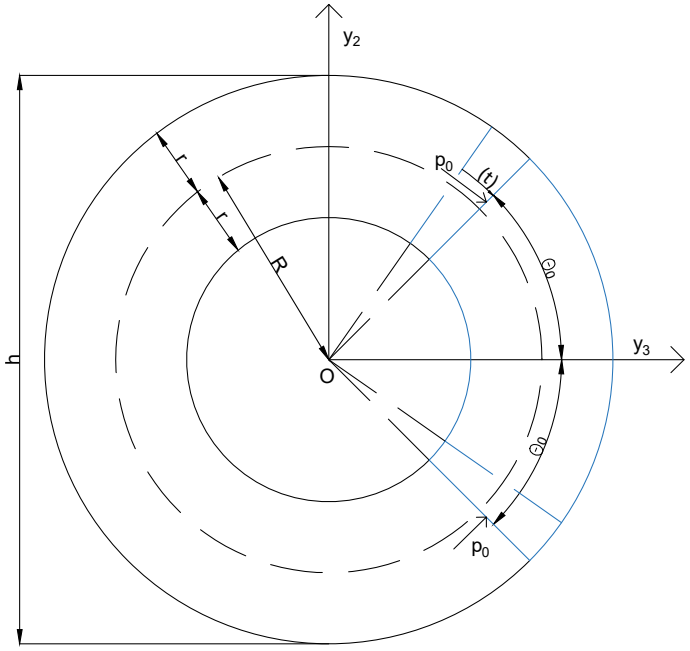

Figure 2.2. Sketch of the geometries for the liquid damper.

r is the inner radius of the of the cross-section of the torus, R is the radius to the center O and $h = 2(R+r)$ is the outer diameter of the damper.

2.2.1 Modelling of the smart-liquid damper

Before describing the fluid, some assumptions is made in order to reduce the complexity of the problem.

- Fluid is incompressible
- Rotating as a physical pendulum around O
- Moving as a connected rigid body
- The pressure on either of the end surfaces is p_0. No gradients is assumed within the oscillating fluid indicated on figure 2.2

The parameter $\theta(t)$ is a degree of freedom to describe the fluid motion with the sign definition seen in figure 2.2, and Θ_0 is a reference value of the movement for the oscillating fluid.

The fluid velocity profile in any section of the moving fluid is assumed to be given as,

$$v(x,t) = v_0(t) \cdot \begin{cases} 2\left(\frac{x}{a} - \frac{1}{2}\left(\frac{x}{a}\right)^2\right) & , \quad 0 \leq x \leq a \\ 1 & , \quad a < x < r \end{cases} \tag{2.1}$$

This assumed velocity profile has been suggested for smart fluids by [Goncalves, 2005].

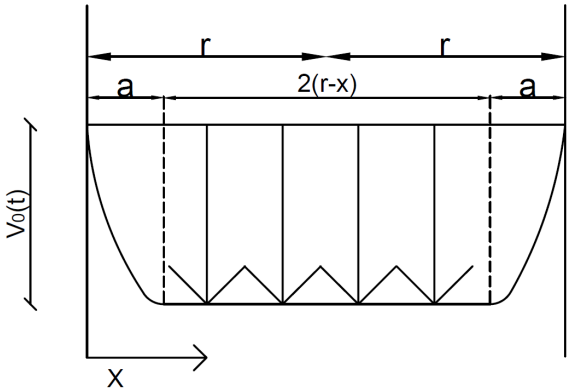

Figure 2.3. Assumed velocity profile.

The velocity profile can be seen in figure 2.3. The indicated velocity profile is assumed to be rotational symmetric, x is a radial coordinate orientated from the inner side of the torus toward the center line. The parameter a indicates the boundary layer thickness, and $v_0(t)$ is the constant fluid velocity, outside the boundary layer. The velocity profile in equation (2.1) presumes that the gradient $\frac{\partial v}{\partial x}$ and hence the shear stress is continuous at the top of the boundary layer at $x = a$.
Based of the indicated assumptions $v_0(t)$ is given as:

$$v_0(t) = R\dot{\theta}(t) \tag{2.2}$$

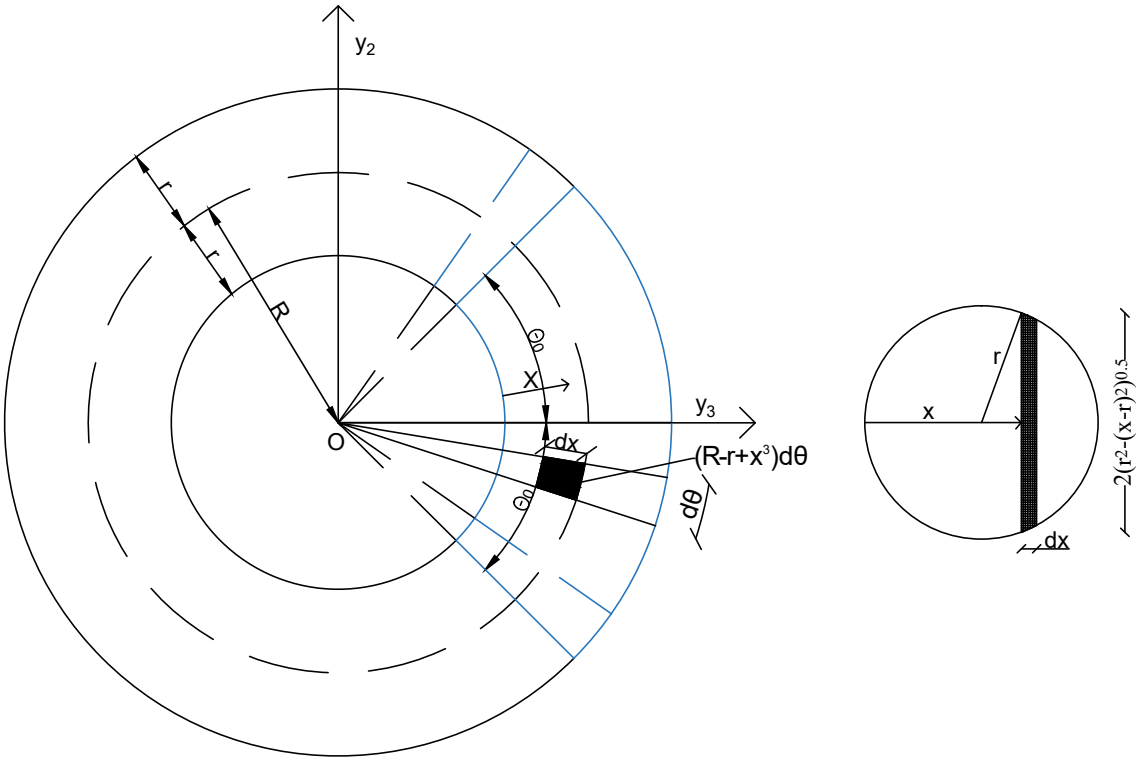

Figure 2.4. Geometries of the damper.

The rotating fluid may be represented as an equivalent mathematical pendulum with the mass m_e and length R_e. The requirements is that the kinetic energy and the potential energy of the physical pendulum (the fluid) and the mathematical pendulum are identical. The kinetic energy of the oscillating fluid is calculated as:

$$T(t) = \int_{-\Theta}^{\Theta}\int_{0}^{r}\frac{1}{2}\rho v^2(x,t)2\pi(r-x)dxRd\theta = \pi r^2R^3\Theta_0\rho\left(1-\frac{14}{15}\frac{a}{r}+\frac{26}{15}\left(\frac{a}{r}\right)^2\right)\dot{\theta}^2(t) \tag{2.3}$$

where ρ indicates the mass density of the fluid which is $\rho \simeq 1000\,\mathrm{kN/m^3}$, for smart fluids it can be found in Chapter 3.

The mass of the oscillating fluid becomes:

$$m = \int_{-\Theta_0}^{\Theta_0}\int_{0}^{2r}\rho(R-r+x)2\sqrt{r^2-(x-r)^2}dxd\theta = \rho 2\pi\Theta_0 r^2R \tag{2.4}$$

The gravity force and centrifugal force is acting in the mass center placed at the distance R_G from the origin O.

$$mR_G = \int_{-\Theta_0}^{\Theta_0}\int_{0}^{2r}\rho(R-r+x)^2 2\sqrt{r^2-(x-r)^2}dxd\theta \Rightarrow R_G = R\left(1+\frac{1}{4}\frac{r^2}{R^2}\right) \tag{2.5}$$

The kinetic energy of the equivalent mathematical pendulum is given as equation (2.6)

$$T(t) = \frac{1}{2}m_eR_e^2\dot{\theta}^2(t) \tag{2.6}$$

Equating the kinetic energy of the equivalent mathematical pendulum to that of the oscillating liquid, the relationship between m_e and R_e follows from (2.7).

$$m_e R_e^2 = mR^2 \left(1 + \frac{3}{4}\left(\frac{r}{R}\right)^2\right) \tag{2.7}$$

In order to facilitate the calculation of the potential energy of the liquid mass, we shall choose R_e as (2.8)

$$R_e = R_G = R\left(1 + \frac{1}{4}\left(\frac{r}{R}\right)^2\right) \tag{2.8}$$

Then, from 2.7 and 2.8, the equivalent mass of the mathematical pendulum is given by equation (2.9)

$$m_e = m\frac{\left(1 + \frac{3}{4}\left(\frac{r}{R}\right)^2\right)}{\left(1 + \frac{1}{4}\left(\frac{r}{R}\right)^2\right)} \tag{2.9}$$

From this the equation of motion for the two degree of freedom system can be set up

2.2.2 Equation of of motion of the 2-DOF model

The velocity component of the primary structure in the moving (x_1, x_2, x_3)-coordinate system can be written as equation (2.10)

$$\left.\begin{aligned} \dot{u}_2(x_3,t) &= -\Omega x_3 - \Phi(x_3)\dot{q}(t) \\ \dot{u}_3(x_3,t) &= -\Omega\Phi(x_3)q(t) \end{aligned}\right\} \tag{2.10}$$

Where Φ is the undamped modeshape, of the blade in the edgewise direction. The fixed frame components in the (X_1, X_2, X_3)-coordinate system of the displacement vector of the center of gravity G for the liquid becomes:

$$\left.\begin{aligned} U_{2,G}(t) &= -x_0 \sin\Psi - a_1 q\cos\Psi - R_e \sin(\Psi + \varphi + \theta) \\ U_{3,G}(t) &= x_0 \cos\Psi - a_1 q\sin\Psi - R_e \cos(\Psi + \varphi + \theta) \end{aligned}\right\} \tag{2.11}$$

The fixed frame components of the velocity vector of the primary structure at the position x_3 becomes:

$$\left.\begin{aligned} \dot{U}_2(x_3,t) &= -(x_0\Omega + a_1\dot{q})\cos\Psi + a_1 q\Omega\sin\Psi - R_e(\Omega + \dot{\varphi} + \dot{\theta})\cos(\Psi + \varphi + \theta) \\ \dot{U}_2(x_3,t) &= -(x_0\Omega + a_1\dot{q})\sin\Psi - a_1 q\Omega\cos\Psi - R_e(\Omega + \dot{\varphi} + \dot{\theta})\sin(\Psi + \varphi + \theta) \end{aligned}\right\} \tag{2.12}$$

Where a_1 and b is defined as auxiliary parameters for the undamped modeshape at the damper location and Ψ indicate the azimuthal angle of the blade defined in Figure 2.5.

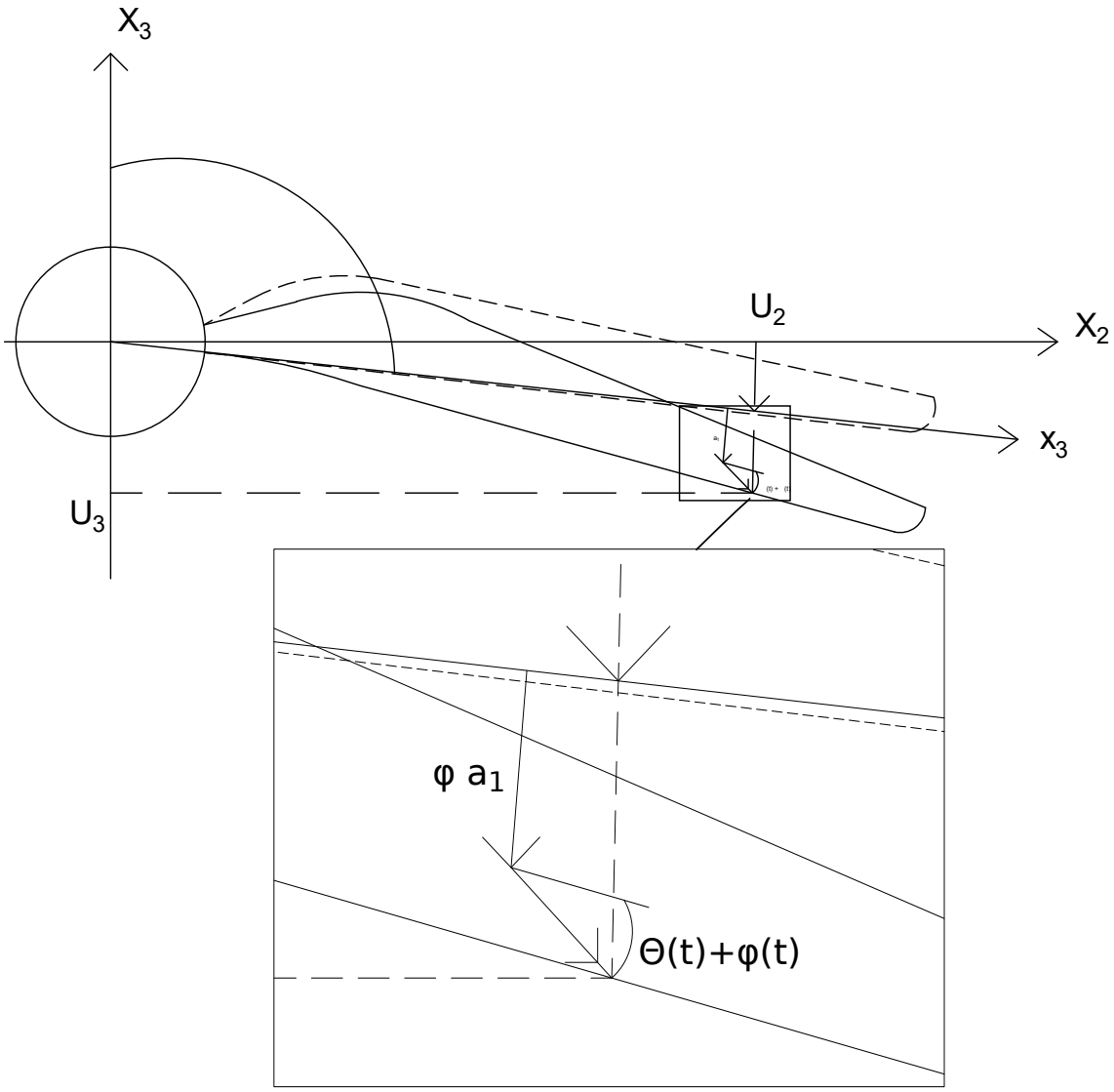

Figure 2.5. Displacement vectors of the 2-DOF system U_2 and U_3.

$$a_1 = \Phi(x_0), \quad b = \Phi'(x_0), \quad \Psi(t) = \omega t, \quad \varphi(t) = bq(t) \tag{2.13}$$

Thus, the total kinetic energy of the 2-DOF system becomes equation (2.14)

$$\begin{aligned} T &= \frac{1}{2}\int_0^L \mu(x_3)(\dot{u}_2^2(x_3,t) + \dot{u}_3^2(x_3,t))dx_3 + \frac{1}{2}m_e(\dot{U}_{2,G}^2(t) + \dot{U}_{3,G}^2(t)) \\ &= \frac{1}{2}m_0(\dot{q}^2 + \Omega^2 q^2) + m_1\Omega\dot{q} + \frac{1}{2}\Omega^2 m_2 \\ &+ \frac{1}{2}m_e(((x_0\Omega + a_1\dot{q})^2 + a_1^2q^2\Omega^2 + R_e(\Omega + b\dot{q} + \dot{\theta})^2 \\ &+ 2R_e(\Omega + b\dot{q} + \theta)((x_0\Omega + a_1\dot{q})\cos(bq+\theta) + a_1q\Omega) + a_1q\Omega\sin(bq+\theta) \end{aligned} \tag{2.14}$$

Where m_0, m_1 and m_2 is defined as modal mass parameter in equation (2.15).

$$\begin{aligned} m_0 &= \int_0^L \mu(x_3)\phi^2(x_3)dx_3 \\ m_1 &= \int_0^L \mu(x_3)\phi^2(x_3)x_3 dx_3 \\ m_2 &= \int_0^L \mu(x_3)\phi^2(x_3)x_3^2 dx_3 \end{aligned} \tag{2.15}$$

The total potential energy of the system is calculated by the use of equation (2.16)

$$U = mg(x_0\cos\Psi - a_1 q\sin\Psi + R_e\cos(\Psi + bq + \theta)) + \frac{1}{2}k_0(t)q^2 \tag{2.16}$$

where g is the acceleration of gravity. The potential energy consists of two terms, where the fluid describes the potential energy for the displaced fluid, and the other which describes the modal strain energy of the cantilever beam for the deformation in the edge wise direction, in this specific case the physical and modal strain energy is identical. The term $k_0(t)$ denotes the modal stiffness of the blade and is given by equation (2.17);

$$k_0(t) = k_e + k_g(t) \tag{2.17}$$

Where k_e and $k_g(t)$ specify the elastic and geometric contributions to the modal stiffness. The term $k_g(t)$ is expressed by equation (2.18).

$$k_g(t) = k_1\Omega^2 - k_2 g\cos(\Omega t) \tag{2.18}$$

The first term indicates the geometrical stiffening due to the centrifugal acceleration, whereas the second term is caused by the variation of the axial forces during the rotation due to the weight of the blade. The parameters k_e, k_1 and k_2 are given by equation (2.19)

$$\left.\begin{aligned} k_e &= \textstyle\int_0^L EI(x_3)\left(\frac{d^2\phi(x_3)}{dx_3^2}\right)^2 dx_3 \\ k_1 &= \textstyle\int_0^L N_1(x_3)\left(\frac{d\phi(x_3)}{dx_3}\right)^2 dx_3 \quad , \quad N_1(x_3) = \int_{x_3}^L \mu(y_3)y_3 dy_3 \\ k_2 &= \textstyle\int_0^L N_2(x_3)\left(\frac{d\phi(x_3)}{dx_3}\right)^2 dx_3 \quad , \quad N_2(x_3) = \int_{x_3}^L \mu(y_3)dy_3 \end{aligned}\right\} \tag{2.19}$$

The fundamental edgewise angular eigenfrequency of the blade when it is in still-stand position is obtained by equation (2.20)

$$\omega_0 = \sqrt{k_e/m_0} \tag{2.20}$$

The equation of motion of the 2-DOF system is obtained from stationary conditions using Euler-Lagrange equations (2.21) and (2.22).

$$\begin{aligned}
&\frac{d}{dt}\left(\frac{\partial T}{\partial \dot{q}}\right) - \frac{\partial T}{\partial q} + \frac{\partial U}{\partial q} = F_0(t) + F_g(t) - c_0\dot{q} \\
&\quad \Rightarrow (m_0 + m_e(a_1^2 + R_e^2 b^2))\ddot{q} + m_e R_e^2 b\ddot{\theta} + (c_0 + c_a)\dot{q} + (k_0 - \Omega(m_0 + M_e a_1^2))q \\
&\quad + m_e R_e(2a_1 b\ddot{q} + a_1\ddot{\theta} - a_1 b\Omega^2 q)\cos(bq+\theta) \\
&\quad - m_e R_e((a_1 - bx_0)\Omega^2 + 2a_1\Omega\dot{\theta}a_1(b\dot{q}+\dot{\theta})^2)\sin(bq+\theta) \\
&\quad - mg(a\sin(\Omega t) + R_e b\sin(\Omega t + bq + \theta)) \\
&\quad = F_0(t) + F_g(t)
\end{aligned} \tag{2.21}$$

$$\begin{aligned}
&\frac{d}{dt}\left(\frac{\partial T}{\partial \dot{\theta}}\right) - \frac{\partial T}{\partial \theta} + \frac{\partial U}{\partial \theta} = -c_d|\dot{\theta}|\dot{\theta} \\
&\quad \Rightarrow m_e R_e^2 b\ddot{q} + m_e R_e^2\ddot{\theta} + c_d|\dot{\theta}|\dot{\theta} + m_e R_e a_1(\ddot{q} - \Omega^2 q)\cos(bq+\theta) \\
&\quad + m_e R_e(2a_1\Omega\dot{q} + \Omega^2 x_0)\sin(bq+\theta) - mgR_e\sin(\Omega t + bq + \theta) \\
&\quad = 0
\end{aligned} \tag{2.22}$$

$c_d|\dot{\theta}|\dot{\theta}$ is the damping term for a damper with an orifice [Basu et al., 2015], where c_d is defined as:

$$c_d = \frac{1}{2}\xi\rho r^2 R^3 \tag{2.23}$$

and ξ is a non-dimensional damping parameter. In the semi-active control the term $c_d|\dot{\theta}|\dot{\theta}$ is replaced by a dissipation mechanism given by another expression which can be seen in Chapter 4. From the Euler-Lagrange equations 2.21 and 2.22 a state variable matrix is constructed with time varying values of:

$$Z = \begin{bmatrix} q(t) \\ \dot{q}(t) \\ \theta(t) \\ \dot{\theta}(t) \end{bmatrix} \tag{2.24}$$

From these state variables the standard variation of the edgewise tip displacement is calculated as:

$$\sigma_q = \sqrt{E[(q - E(q))^2]} \tag{2.25}$$

where as $E(q)$ is the mean value of the tip displacement. The standard deviation of the tip displacement is the value sought to reduce as much as possible.

Smart liquids 3

In this chapter the theory and characteristics of the smart liquids are presented, as well as the constitutive models used to describe the fluids.

When talking about smart materials, it implies that the material can change its properties due to external exposure of:

- Mechanical
- Electrical
- Magnetic

[Reece, 2006]

Smart liquids has different applications. As an example it is used in car suspensions systems, where it is used to control how stiff/soft the suspension should be depending on the surface that is driven on [Goncalves, 2005].

In this project the use of smart liquids is to change specific properties to enhance the performance of the liquids damping capabilities. To do this, a fluid which uses magnetic fields to change its properties, is examined to see the effectiveness of using this material as damping material.

The liquid used in this project is magneto-rheological fluids. The fluid will be referred to as MR-fluids in the project. The fluid response time to the magnetic field is 2-3 orders of magnitude smaller than any eigenperiod of significance to the structural response. Hence the control can be considered without any delay effect, which enhance the stability and efficiency of the control.

The downside to the fluids is that its relatively new area that needs more exploring, so models is not that refined yet. Also they are quite expensive to acquire. Further the fluid itself consists of small particles suspended in the carrier fluid, they do settle at some point if not kept in motion. The settling problem should only be a problem if the wind turbine is at stand still position, under transportation or not during normal operation.

3.1 MR-liquids

MR-liquids consists of a lot of very small magnets suspended in a carrier liquid. By introducing a magnetic field to the liquid the small magnets form strings in the direction of the magnetic field as show in figure 3.1 and 3.2, where an "off" state and "on" state is shown for the liquid.

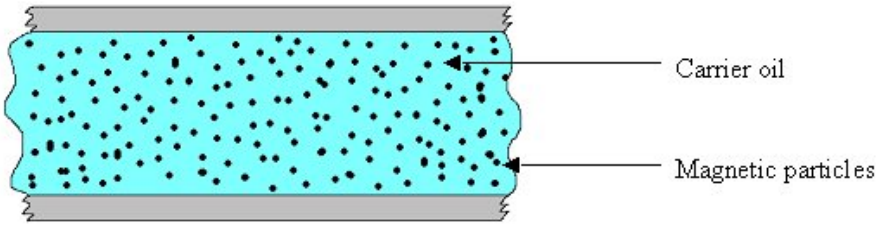

Figure 3.1. MR-liquid in its "off" state [Wikipedia, 2017].

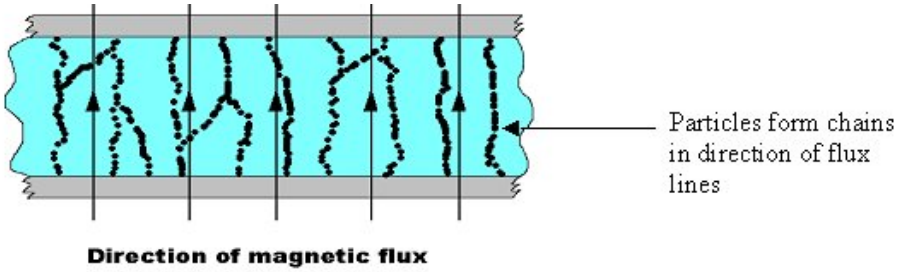

Figure 3.2. MR-liquid in its "on" state. [Wikipedia, 2017].

Figure 3.3 shows a circular damper of radius R with a coil, of the circumference length $L = 2R\Theta_0$ covering a fluid confined within the center angle $2\Theta_0$. The coil produces a magnetic field of the strength H. E is the voltage of the power supplied which produces the current in the coil, which can be changed to vary the magnitude of the electric field according to Faraday's law. In this case the magnetic field is directed in the circumference direction.

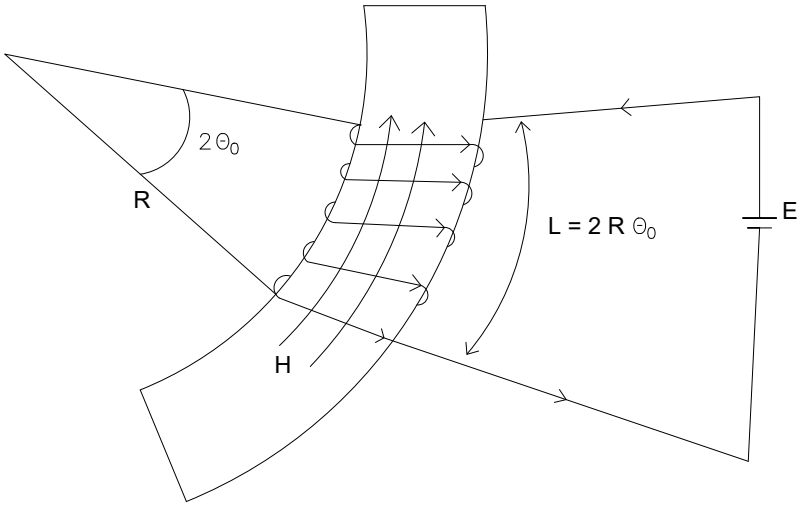

Figure 3.3. Principle sketch of a part of the torus with wires to create an electromagnetic field.

The strings of the aligned magnets formed in Figure 3.2 will restrict the motion of the fluid and through that increase the viscous properties of the fluid. The energy needed to yield the strings is then controlled by the magnitude of the applied magnetic field [Mark R. Jolly, 2000].

The benefits of using this MR-fluid is the control it offers for the yield stress and viscosity of the fluid. As mentioned the response time to magnetic field is instant and is reversibly. The specific fluid information can be found Table 3.1 which is from [Lord Corporation, 2011].

Table 3.1. Fluid characteristics for the specific MR-fluid MRF-132DG, $H = 0$.

μ_{MR}	0.112 ± 0.02 $[Pa \cdot s]$
ρ_{MR}	2950-3150 $[kg/m^3]$

In order to use this liquid for calculations, a model for the liquid is needed, to describe the characteristics in terms of a functional relation between the fluid parameters and the applied H-field. Also a velocity profile is needed which is assumed to follow figure 2.3.

With a velocity profile assumed a constitutive model for the liquid is needed as well. The Bingham model can be seen in equation 4.10.[Goncalves, 2005] indicates the following empirical model for the dependency of the shear stress τ_0 on the magnetic field H.

$$\tau_0 = C \cdot 271700 \cdot \Phi_1^{1.5239} \cdot \tanh(6.33 \cdot H) \tag{3.1}$$

Where:

C	Constant dependent on carrier fluid
H	Strength of the magnetic field
Φ_1	Magnetic flux

Unfortunately the units of the parameters i Equation 3.1 were not indicated by the author. According to [Jiles, 1998] Φ_1 is usually referred to as the magnetic flux measured in webers which also is $Wb = \frac{kgm^2}{s^2A}$. If looking at the equation 3.1 estimated emperically through an experiment, it would seem to end with a single max value of τ_0, which means the curve goes asymptote towards a value. Known from [Lord Corporation, 2011] the fluid MRF-132DG's carrier fluid is hydrocarbon oil which according to [Goncalves, 2005] is corresponding to a value of $C = 1$. Because of the uncertainty around the experimental formula from [Goncalves, 2005] another option is available. [Lord Corporation, 2011], indicates experimental results, which have been smoothed with a 2nd polynomial fit.

The digitalized plot can be seen in Figure 3.4.

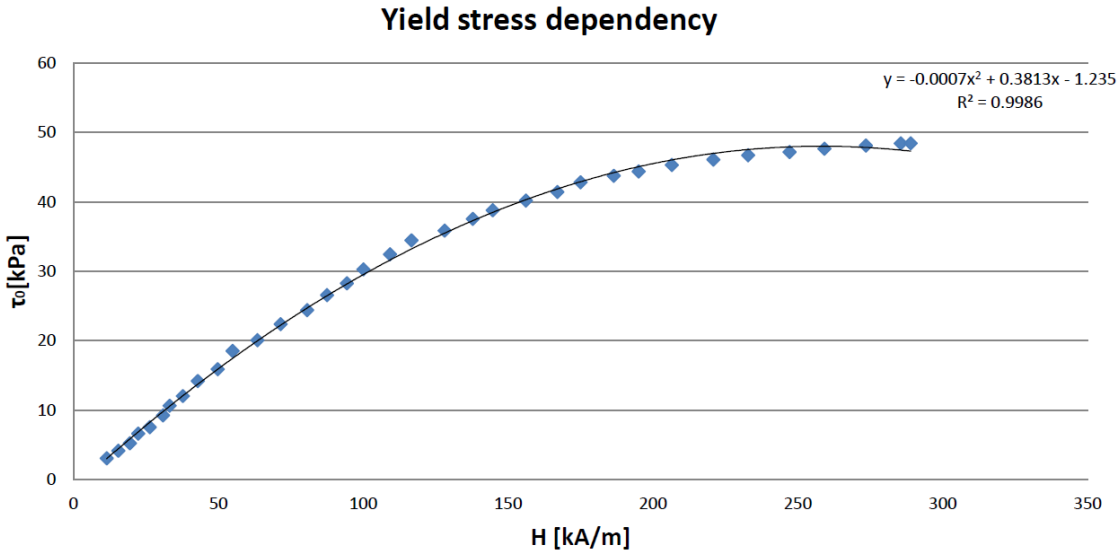

Figure 3.4. The yield stress dependency on the magnetic field strength [Lord Corporation, 2011].

From this it can be seen a second degree polynomial relative precise can describe the connection between the yield stress and magnetic field in a given range of operation. The model is then:

$$\tau_0 = -0.0007H^2 + 0.3813H - 1.235 \tag{3.2}$$

where τ_y is in kPa and H is in $\frac{kA}{m}$. It is important to know this only concerns this particular fluid, as there is numerous ways to create the the MR-fluid for specific needs.

It has not been possible to find a model that covers the change of the viscosity with altering the magnetic field.

Semi-active control 4

In this chapter the semi-active control is presented with control law for both the orifice and smart liquid.

As the idea is to control the motion of the oscillating smart fluid via the damping capabilities, a control law is needed indicating the dependency of the fluid parameters on the state variables defining the primary structure and the damping device. In this project a semi-active control is used, which is going to be implemented through a feedback control system. The smart fluid is modelled to control the yield strength and viscosity of the liquid, such when the liquid is moving, it exerts an inertial force that counter act the vibration of the primary structure. This is controlled through a magnetic field, which alters the viscosity and the yield strength of the liquid.

Before the semi-active control based on smart fluids is outlined, a preliminary analysis has been carried out to investigate, whether the performance of the damping model in equation 2.23 can be improved by a semi-active control via the parameter $\xi = \xi(t)$. Physically ξ may be considered as a proportional change of the area of the opening in the orifice.

4.1 Orifice control

The term $c_d|\dot{\theta}|\dot{\theta} = c_d\dot{\theta}^2(t)sign(\dot{\theta})$ in equation 2.22 is suppose to model the energy dissipation due to an orifice device. c_d is given in equation 2.23.

In its most general form $\xi(t)$ is taken on the form of the following feed back control law:

$$\xi(t) = \xi_0 + \xi_c(q, \theta, \dot{q}, \dot{\theta}) \tag{4.1}$$

where ξ_c is a function of the state variables of the system. The value of ξ_0 is taken as the optimal value used for passive control which has been estimated to be $\xi_0 = 5.68$ by [Basu et al., 2015].
The equation of motion for the reduced 2-DOF system is given by equations 2.21 and 2.22. The dissipative effect of the damper on the primary structure is via the inertial term $m_e R_e^2 b\ddot{\theta}$ in equation 2.21. Hence, this term should be in phase with the velocity $\dot{q}$ of the primary structure. Damping of the primary structure then takes place whenever, if:

$$\ddot{\theta}(t)sign(\dot{q}) > 0 \tag{4.2}$$

An instantaneous increase of $\xi(t)$, and hence $c_d|\dot{\theta}|\dot{\theta}$, has to be balanced by the acceleration terms $m_e R_e^2 \ddot{\theta}$ and $m_e R_e^2 b\ddot{q}$ in equation 2.22, since the other terms remains almost unchanged. Since the control is performed in the equation of motion for the angle $\theta(t)$, it is in the following analysis assumed that $\ddot{\theta}(t)$ is the most crucial parameter. Then under semi-active control activation the following relation must be fulfilled:

$$m_e R_e^2 \ddot{\theta} + c_d \dot{\theta}^2(t) sign(\dot{\theta}) \simeq 0 \Rightarrow \ddot{\theta} + l(t)\xi(t) sign(\dot{\theta}) \simeq 0 \tag{4.3}$$

where:

$$l(t) = \frac{1}{2} \frac{\rho r^2 r^3}{m_e R_e^2} \dot{\theta}^2(t) \tag{4.4}$$

Obviously $l(t) \geqslant 0$.
The control law is taken on the form:

$$\xi(t) = \xi_0 - \xi_1 sign(\dot{\theta}(t)) sign(\dot{q}(t)) \tag{4.5}$$

The second term on the right hand side represents the semi-active component of the control effect where ξ_1 is a non-dimensional gain factor. To ensure that the semi-active component overrules the passive component under oscillation, it is required that:

$$|\xi_1| >> \xi_0 \tag{4.6}$$

Then under semi-active control equation 4.5 is reduced to:

$$\xi(t) \simeq -\xi_1 sign(\dot{\theta}) sign(\dot{q}) \tag{4.7}$$

Insertion of equation 4.7 into equation 4.3 provides:

$$\ddot{\theta} \simeq l(t)\xi_1 sign(\dot{q}(t)) \tag{4.8}$$

Then, equation 4.2 is fulfilled, if equation 4.3 and 4.5 is fulfilled, and:

$$\xi_1 > 0 \tag{4.9}$$

With this model in use, response of the state variables are represented graphical for varying values of ξ_1 in the following figures 4.1, 4.2, 4.3, 4.4, 4.5 and 4.6.

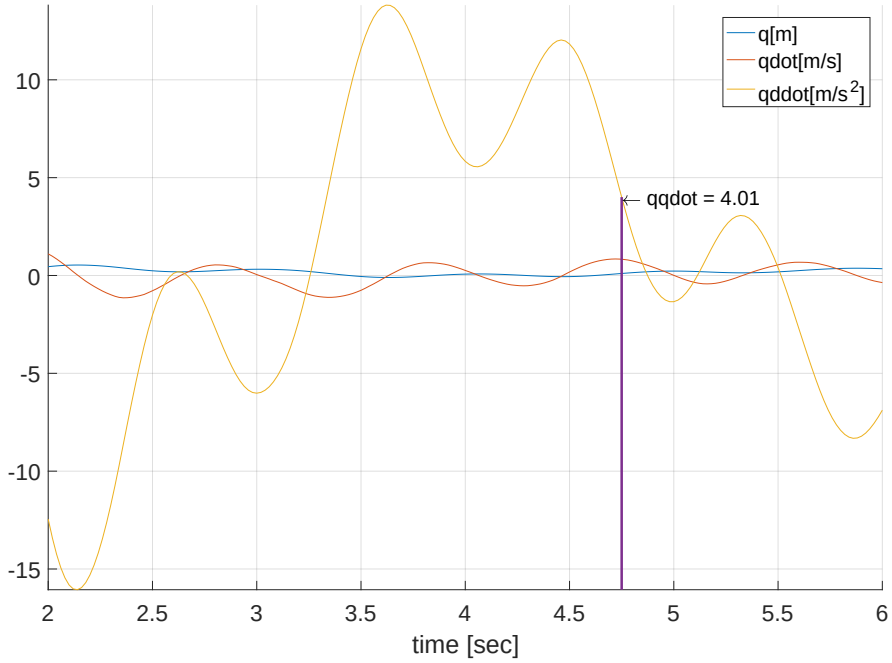

Figure 4.1. Timeseries of $q, \dot{q}, \ddot{q}$ with $\xi_1 = 0$.

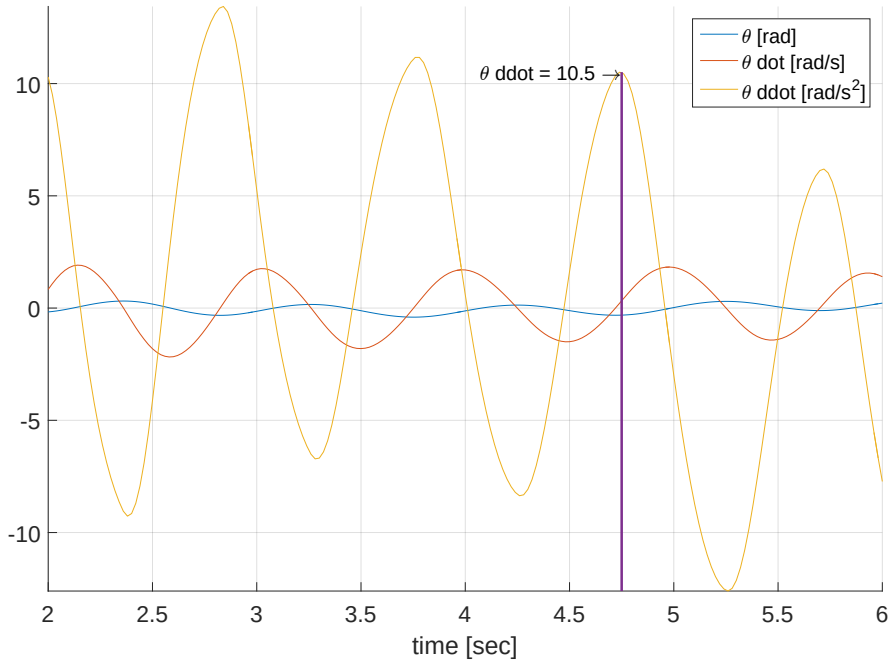

Figure 4.2. Timeseries of $\theta, \dot{\theta}, \ddot{\theta}$ with $\xi_1 = 0$.

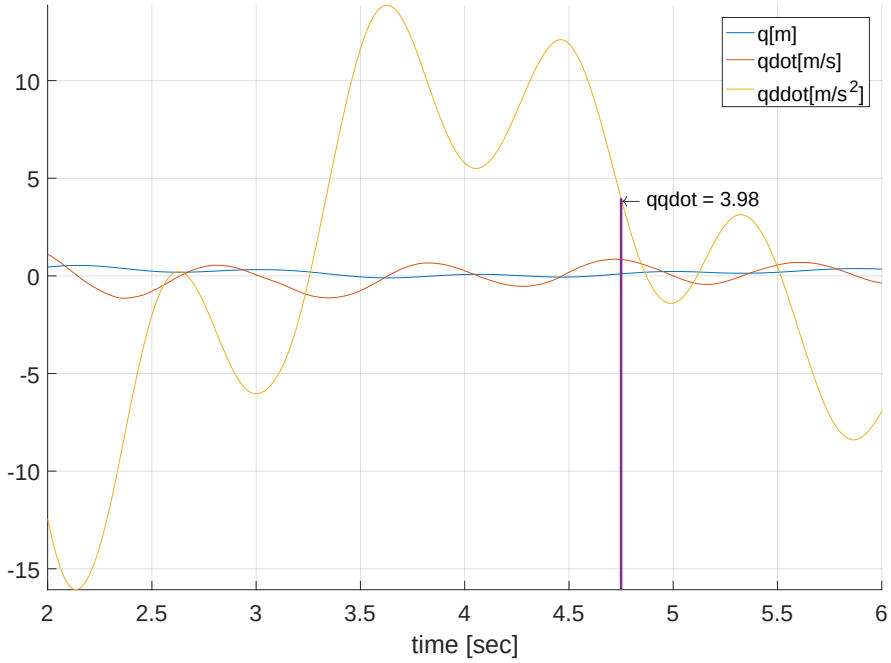

Figure 4.3. Timeseries of $q, \dot{q}, \ddot{q}$ with $\xi_1 = 10$.

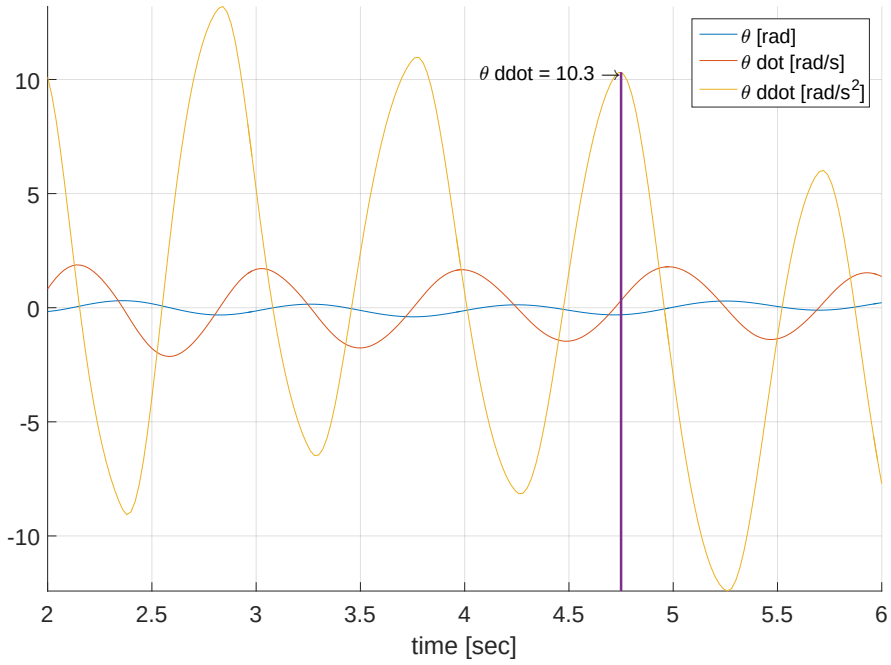

Figure 4.4. Timeseries of $\theta, \dot{\theta}, \ddot{\theta}$ with $\xi_1 = 10$.

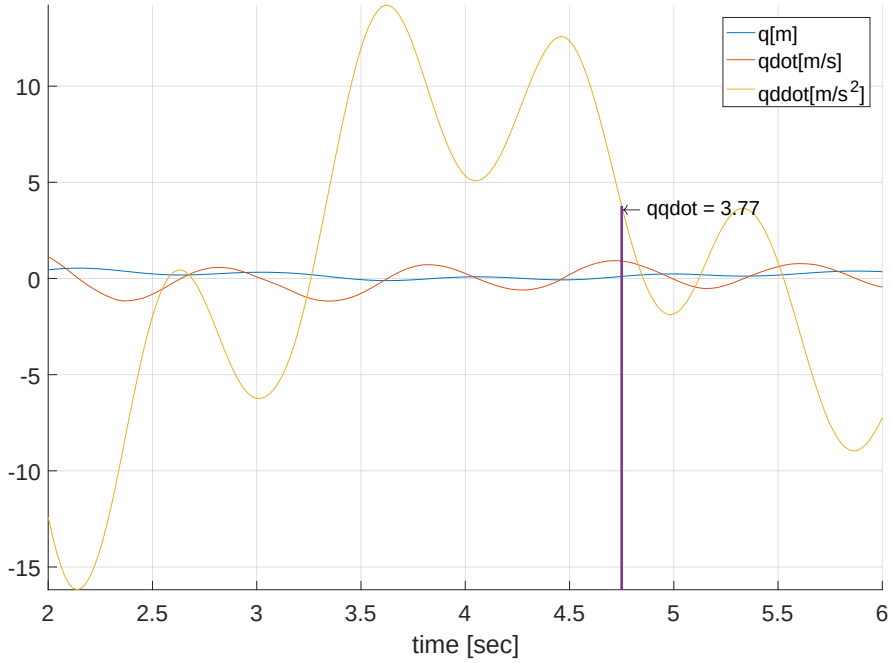

Figure 4.5. Timeseries of $q, \dot{q}, \ddot{q}$ with $\xi_1 = 100$.

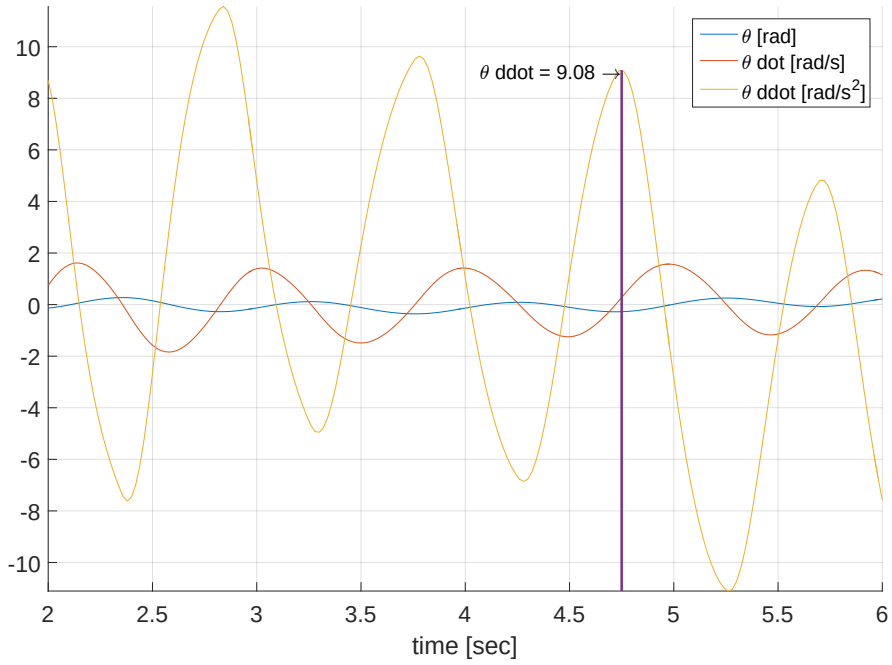

Figure 4.6. Timeseries of $\theta, \dot{\theta}, \ddot{\theta}$ with $\xi_1 = 100$.

As can be seen in figures 4.1 - 4.6 $\ddot{\theta}$ and $\dot{q}$ are in phase for any values of ξ, so the system is optimal tuned for nearly optimal tuned for all values of ξ. Of course the same wind load on the structure is applied in all three cases. On the figures the values of $\ddot{\theta}$ and $\ddot{q}$ have been marked for $t = 4.75\,\text{sec}$. It is seen that $\ddot{\theta}$ decreases from $10.5\,\text{rad/s}^2$ down to $9.08\,\text{rad/s}^2$ for values of $\xi_1 = 1, 10, 100$, whereas the $\ddot{q}$ decreases from $4.01\,\text{m/s}^2$ to $3.77\,\text{m/s}^2$. This means the assumption that $\ddot{\theta}$ is the crucial acceleration term in equation 2.21 is wrong, and $\ddot{q}(t)$ is equally important. In order to make the semi-active control work for the orifice control $\ddot{\theta}$ should increase.
The semi-active orifice control should merely be applied to change the parameter $\xi_0 = \xi_0(\Omega)$ for optimal tuned control under changing rotational speed Ω of the rotor.

4.2 Smart fluid control

The idea is to formulate a model for the viscosity of the fluid as well with the dependency on the magnetic field. For this a velocity profile and a yield stress distribution is needed. Where [Goncalves, 2005] has been used for the velocity profile $v(x,t)$ which can be seen in figure 2.3, and the yield stress distribution can be seen in the following equations which follows the Bingham model, which is suited for use when modelling smart fluids [Goncalves, 2005], [Mark R. Jolly, 2000].

$$\tau(x,t) = \tau_y(t) + \mu(t)\frac{\partial v(x,t)}{\partial x} \tag{4.10}$$

With this model the shear stress distribution becomes:

$$\tau(x,t) = \begin{cases} \tau_y(t)sign(v_0(t)) + \mu(t)\frac{v_0(t)}{a}\left(1-\frac{x}{a}\right) & , \quad x \le a \\ \tau_y(t)sign(v_o(t)) & , \quad a < x \le r \end{cases} \tag{4.11}$$

The following linear feed back control laws are assumed for the $\mu(t)$ and $\tau_y(t)$ of the fluid:

$$\mu(t) = \mu_0 + \mu_1\frac{q(t)}{q_0} + \mu_2\frac{\theta(t)}{\theta_0} + \mu_3\frac{\dot{q}(t)}{q_0\omega_1} + \mu_4\frac{\dot{\theta}(t)}{\theta_0\omega_1} \tag{4.12}$$

$$\tau_y(t) = \tau_0 + \tau_1\frac{q(t)}{q_0} + \tau_2\frac{\theta(t)}{\theta_0} + \tau_3\frac{\dot{q}(t)}{q_0\omega_1} + \tau_4\frac{\dot{\theta}(t)}{\theta_0\omega_1} \tag{4.13}$$

The right-hand side of equation 4.12 and 4.13 should be considered as control demands. Based on measured values of the state variables the value of $\mu(t)$ and $\tau_y(t)$ can be specified. Next the required value is applied to $\mu(t)$ and $\tau_y(t)$ of the magnetic field. q_0 and θ_0 are arbitrary selected normalization values chose as $q_0 = 0.5\,\text{m}$, $\theta_0 = \frac{\pi}{10}$ and ω_1 is the fundamental edgewise eigenfrequency of the wind turbine blade. The normalizations insure that the parameters $\mu_0...\mu_4$ and $\tau_0...\tau_4$ should be of the same order of magnitude. The influence of the parameters $\mu_0...\mu_4$ and $\tau_0...\tau_4$ on the standard deviation σ_q of the blade will be determined by independent variation of the parameters.

The dissipation component in equation 2.22, namely the $c_d|\dot{\theta}|\dot{\theta}$, is in this investigation replaced with an equivalent dissipation mechanism $c(\dot{\theta})$, determined below.
The energy absorbed by $c(\dot{\theta})\dot{\theta}$ must balance the dissipated energy in the fluid per unit of time. The dissipation per unit of time in a unit volume is given as $\tau\frac{\partial v}{\partial x}$, where τ is the shear stress and

$\frac{\partial v}{\partial x}$ is the velocity gradient. Then the following relation applies:

$$\begin{aligned} c(\dot{\theta})\dot{\theta} &= \int_{-\Theta_0}^{\Theta_0}\int_0^r 2\pi x dx R d\theta \tau_y \left(\frac{\partial v}{\partial x}\right) \\ &= 4\pi R^2 \Theta_0 \int_0^a x\left(1-\frac{x}{a}\right)\left(\tau_y sign(\dot{\theta}) + \mu\frac{R}{a}\left(1-\frac{x}{a}\right)\dot{\theta}\right) dx\,\dot{\theta} \\ &= (c_1 sign(\dot{\theta}) + c_2\dot{\theta})\dot{\theta} \Rightarrow \\ c(\dot{\theta}) &= c_1 sign(\dot{\theta}) + c_2\dot{\theta} \end{aligned} \tag{4.14}$$

Where the coefficients $c_1(t)$ and $c_2(t)$ are given as:

$$\begin{aligned} c_1(t) &= \frac{2}{3}\pi\Theta_0 a R^2 \tau_y(t) \\ c_2(t) &= \frac{1}{3}\pi\Theta_0 R^3 \mu(t) \end{aligned} \tag{4.15}$$

Then the next to do, is to determine the influence of $\tau_y(t)$ and $\mu(t)$ on the state vector components by varying the parameters in Equation 4.12 and 4.13 as assembled in the vectors $\overline{\tau}$ and $\overline{\mu}$ given as.

$$\overline{\tau} = \begin{bmatrix} \tau_0 \\ \tau_1 \\ \tau_2 \\ \tau_3 \\ \tau_4 \end{bmatrix}, \qquad \overline{\mu} = \begin{bmatrix} \mu_0 \\ \mu_1 \\ \mu_2 \\ \mu_3 \\ \mu_4 \end{bmatrix} \tag{4.16}$$

The analysis is preformed so the parameters are individually changed in order to see the influence on the vibration level of the primary system as measured by the standard deviation σ_q. To give an example in figure 4.7 where the effect of μ_1 is analyzed by setting it to a range of values, will the rest of the model parameters set to zero:

$$\overline{\tau} = \begin{bmatrix} 0 \\ 0 \\ 0 \\ 0 \\ 0 \end{bmatrix}, \qquad \overline{\mu} = \begin{bmatrix} 0 \\ \mu_1 \\ 0 \\ 0 \\ 0 \end{bmatrix} \tag{4.17}$$

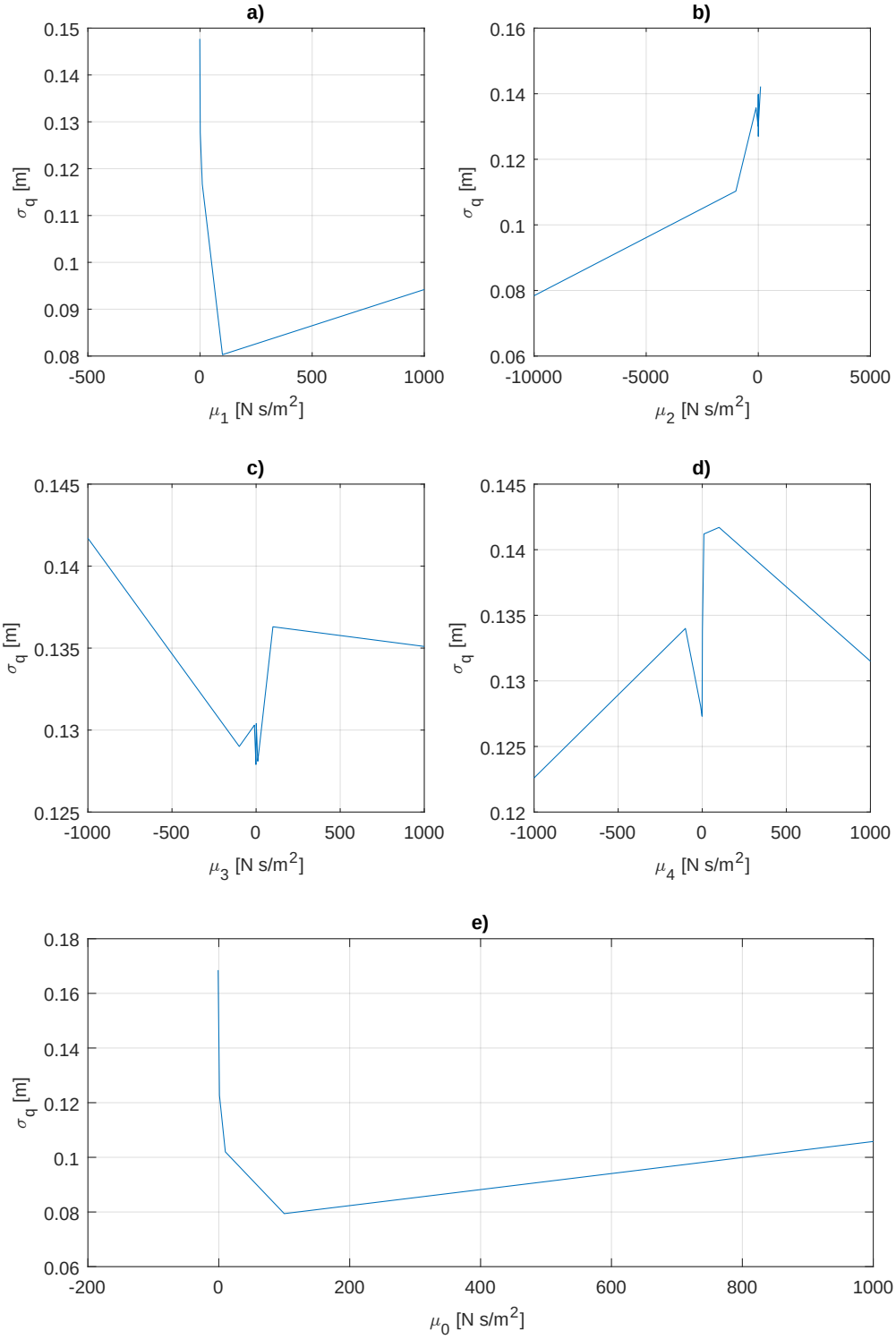

Figure 4.7. Variation of σ_q with components in $\overline{\mu}$, $\overline{\tau} = 0$.

As seen in Figure 4.7a and 4.7e the minimum value of $\sigma_q = 0.08\,\mathrm{m}$ are obtained for both case for $\mu_0 = \mu_1 = 100\,\mathrm{Ns/m^2}$. Based on the applied normalization in Equation 4.12 the physical meaningful variational interval of the parameters μ_2, μ_3, μ_4 should be say $[-400\,\mathrm{Ns/m^2}, 400\,\mathrm{Ns/m^2}]$. In this interval the minimum value is attained for $\mu_2 \simeq \mu_3 \simeq \mu_4 \simeq 0\,\mathrm{Ns/m^2}$.

In all three cases the minimum value is above $\sigma_q = 0.08\,\mathrm{m}$. Hence, it may be concluded that these three terms should be excluded, so Equation 4.18 reduced to:

$$\mu(t) = \mu_0 + \mu_1 \frac{q(t)}{q_0}, \qquad \mu_0 = \mu_1 = 100\,\mathrm{Ns/m^2} \tag{4.18}$$

For the indicated combined model the standard deviation of the primary structure becomes:

$$\sigma_q = 0.0819\,\mathrm{m} \tag{4.19}$$

Apparently the combination of μ_0 and μ_1 is not reducing the standard deviation σ_q further below the optimal value obtained from μ_0 and μ_1 independently . The same analysis is made for $\overline{\tau}$ as well.

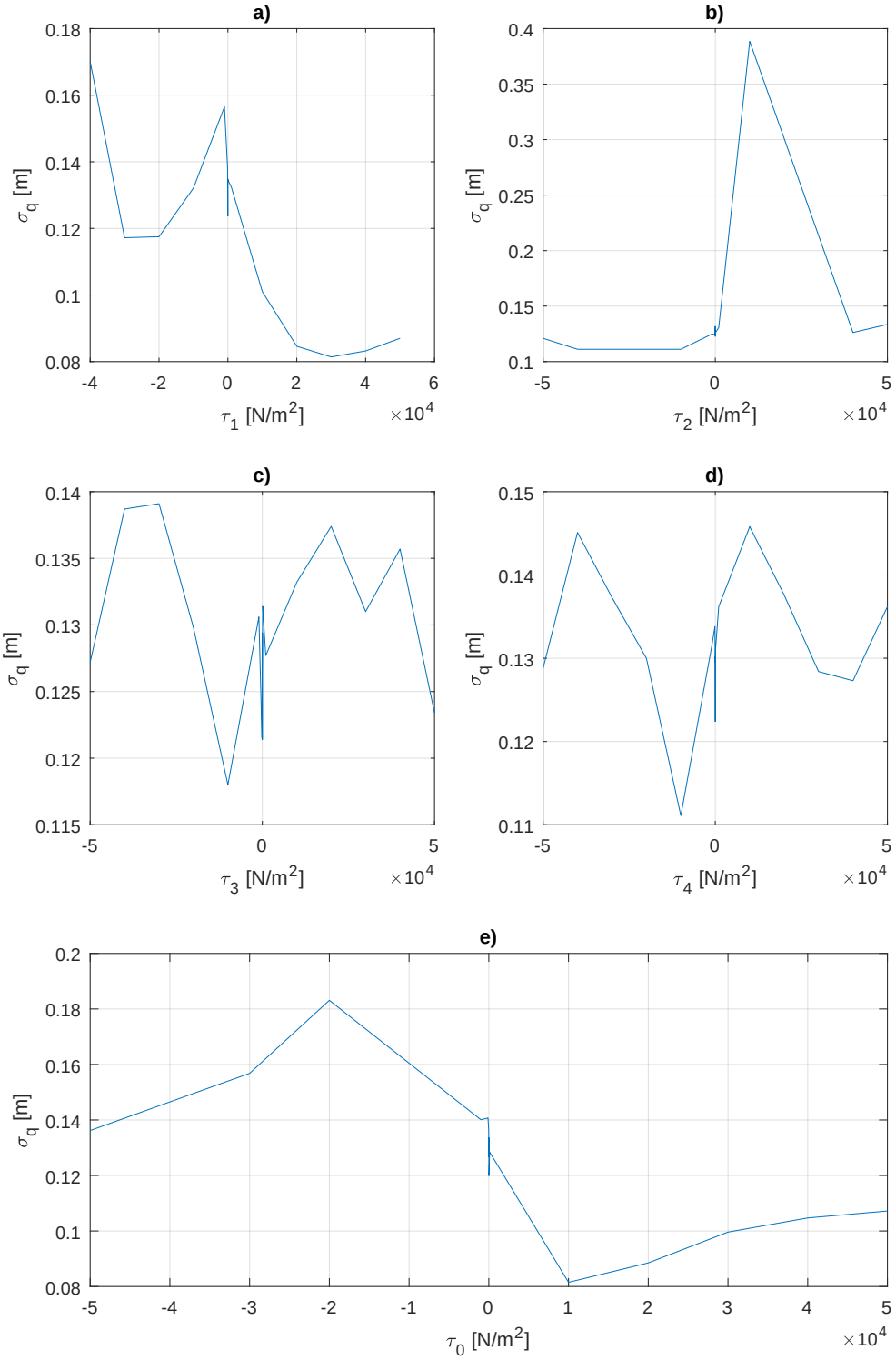

Figure 4.8. Variation of σ_q with components in $\overline{\tau}$, $\overline{\mu} = 0$

From Figure 3.4 it is seen the attainable values of for values in vector $\overline{\tau}$, which is the reason why the interval is much wider here than for $\overline{\mu}$. In Figure 4.8a and 4.8e the minimum value of the standard deviation $\sigma_q \simeq 0.08\,\text{m}$. It seems to follow the same pattern as for $\overline{\mu}$ where the rest of the parameters τ_2, τ_3, τ_4 do not contribute to reduce the standard deviation. The minimum values is for $\tau_0 = 10000\,\text{Pa}, \quad \tau_1 = 30000\,\text{Pa}$.
This would suggest to make the same reduction for Equation 4.13 as done for 4.18. Therefore the following model for $\tau(t)$ is used:

$$\tau_y(t) = \tau_0 + \tau_1 \frac{q(t)}{q_0} \tag{4.20}$$

For the indicated model the standard deviation of the primary structure becomes:

$$\sigma_q = 0.0900\,\text{m} \tag{4.21}$$

As before for the viscosity model the standard deviation is calculated with only the shear stress as a damping factor for this particular result. As seen the result is still not better that the optimized passive controller which is why a possible combination of the two could yield a better result, which will be investigated in the following.

With all the model parameters described, the model parameters can be determined. When doing this two models will be suggested, where one will consist of the values which individually corresponds to the lowest standard deviation of the edgewise tip displacement, and another model which consists of values to achieve a lower over all standard deviation of the tip displacement when looking at the model parameters together. The two models can be seen in equation 4.22 and 4.23.

Model A :

$$\overline{\tau} = \begin{bmatrix} \tau_0 \\ \tau_1 \end{bmatrix} = \begin{bmatrix} 10000 \\ 30000 \end{bmatrix} \frac{N}{m^2}, \quad \overline{\mu} = \begin{bmatrix} \mu_0 \\ \mu_1 \end{bmatrix} = \begin{bmatrix} 100 \\ 100 \end{bmatrix} \frac{Ns}{m^2}, \quad \sigma_q = 0.0995\,\text{m} \tag{4.22}$$

Model B :

$$\overline{\tau} = \begin{bmatrix} \tau_0 \\ \tau_1 \end{bmatrix} = \begin{bmatrix} 0 \\ 0 \end{bmatrix} \frac{N}{m^2}, \quad \overline{\mu} = \begin{bmatrix} \mu_0 \\ \mu_1 \end{bmatrix} = \begin{bmatrix} 15 \\ 125 \end{bmatrix} \frac{Ns}{m^2}, \quad \sigma_q = 0.0782\,\text{m} \tag{4.23}$$

The primary reason of model B is to show that the individual values of the vector entries in $\overline{\tau}$ and $\overline{\mu}$ which yields the smallest standard variation of the tip displacement, does not necessarily yield the smallest value when combined. This can be solved by optimization, this was not done due to limited time.

With these values the standard deviation for the tip displacements is $\sigma_q = 0.0782\,\text{m}$. Based on the performed analysis this was the optimal solution obtained by the semi-active control. As seen, the results is only marginally better than for the passive orifice control, $\sigma_q = 0.0784\,\text{m}$. As a wind turbine does not run with the same rotational speed all the time, a parametric analysis is made upon this parameter as it has a great influence in the systems stiffness and required damping. Therefore it will be analyzed in chapter 5 to see how the incorporated semi-active control system works when the rotational speed changes.

There is still one variable which is of concern and not analysed yet, which is the boundary layer thickness a_1. Because the knowledge is limited to whether what the magnitude this parameter should be, a parameter variation is made, to see what values would be optimal, which can be seen in chapter 5.

Results and Discussion 5

In this chapter the results of the numerical models will be discussed, and a parameter variation made to see which parameters have influences on the dynamics of the system.

From chapter 4 it can be seen that the implementation of semi-active control for the orifice control on the 2-DOF system did not yield any results that would be marginally better than the already optimized passive control system. For the smart fluid control where the use of semi-active control seemed as the best solution, no meaningful change from the optimized passive controller in the standard deviation for the edgewise tip displacement was seen.

From the spectrum it can be seen the effectiveness of the smart fluid control in figure 5.1 which means it works, but it is a variable alternative to the passive control, but it is quite expensive to implement in the wind turbine wing. A more noticeable difference between the orifice control and smart fluid control is the fluid density. For the orifice control is made for water with a density $\rho_{water} \approx 1000\,\text{kg/m}^3$ where as the smart fluid is made for the actual smart fluid which has a density $\rho_{MR} \approx 3000\,\text{kg/m}^3$. This causes the actual mass of the fluid oscillating to be vastly different from the two analysis when assumed the same volume is used, therefore the the two methods is not directly comparable either.

For the model used in smart fluid control it can be seen in figure 4.7 and 4.8, the parameters $\tau_2, \tau_3, \tau_4, \mu_2, \mu_3, \mu_4$ which depends on the velocity terms do not create a meaningful effect on the over all terms of $\tau_y(t)$ and $\mu(t)$, which is why the models is reduced, when the displacement state variables makes the greater change for a reduction in the standard deviation σ_q, which in the end gives the models in Equation 4.22 and 4.23.

In Figure 5.1 the angular frequencies can be seen with the smart fluid damping model in place. It can be seen at the eigenfrequency for the blade that with the damper a large reduction takes place which is needed. But in the lower frequencies a peak still happens which is caused by the turbulence in the wind. This is not being reduced by the damper, since the damper type does not cover low frequency excitation which can be seen in Figure 5.2 with the frequency not changing with the damper in place.

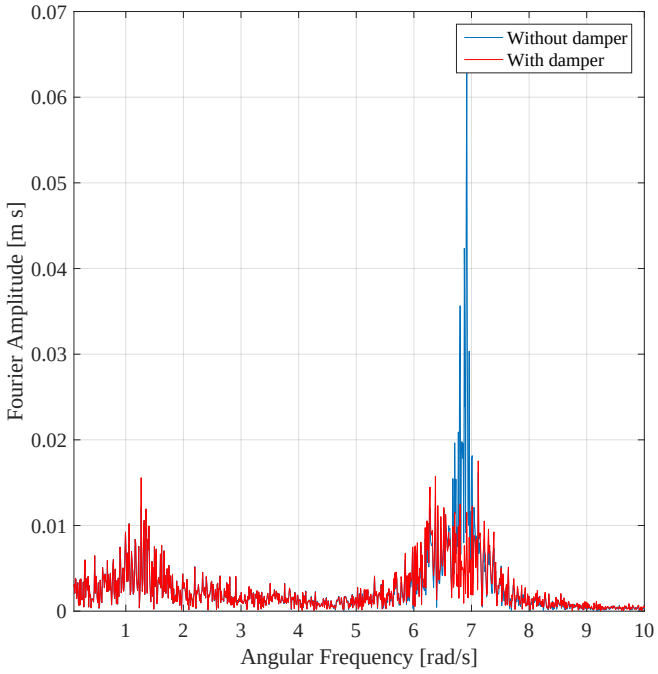

Figure 5.1. Frequencies for the wind turbine wing, with and without the damper in place.

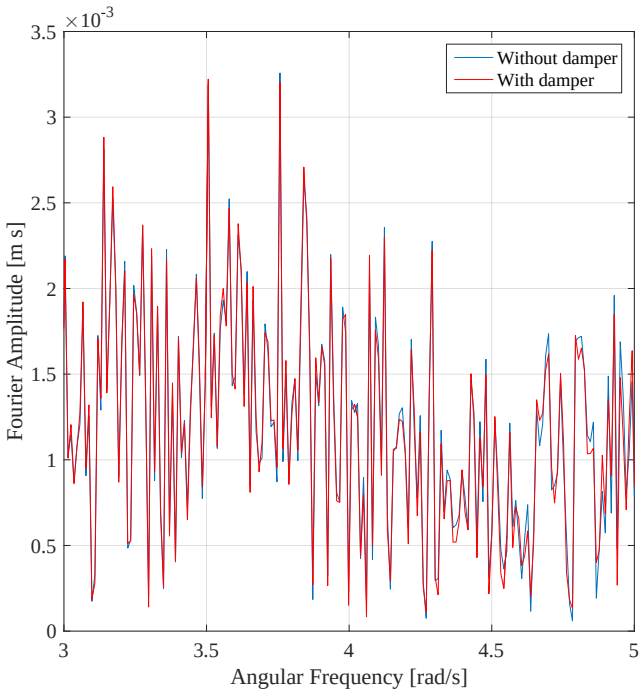

Figure 5.2. Frequencies in between the peaks, where the damper signal follows the undamped.

What is interesting would be to see what would happen if the rotational velocity changes. How would the passive control then react, and could the semi-active control be made adaptable through

either orifice control, smart fluid control or maybe both. A change in Ω causes a detuning of the damper which reduces the effectiveness of the damper, because the centrifugal stiffness of the wind turbine blade. This is what the semi-active control is handling by changing the values of $\overline{\tau}$ and $\overline{\mu}$. Because this could be the key to make the semi-active control work, it is investigated through a parameter variation how different the damping may need to be for different values of the rotational velocity of the rotor.

5.1 Parameter variation

In this section a study on two parameters is showed, which covers the study of the boundary layer thickness a which can be seen in figure 2.3. A variation on the parameter Ω is also done to prove that semi-active control through a feedback control, do have some useful features that is worth exploring. The analysis of Ω is done for the smart fluid control to see if there is any noticeable difference, which should determine the if semi-active control is worth implementing in the wind turbine blade.

5.1.1 Boundary layer thickness

Because the limited knowledge about the parameter a a parametric study has been made to analyse the changes impact on the standard deviation for the tip displacement. This should give an indication of what the optimal value is.
This variation is made for a specific Ω, which has a significant impact on the stiffness of the system. Therefore an analysis is made to show what happens at different values of Ω. The idea of using these smart materials should be, that it can be tuned to different situations to have optimal damping always. Therefore in cases of cut-in and cut-out and pitching, the tuning of the with passive control might not be beneficial for the system during these situations.

The constant values can be seen in Table 5.1.

Table 5.1. Constant values used for the parameter variation.

μ	0.1 $[Pa \cdot s]$
τ_y	100 $[Pa]$

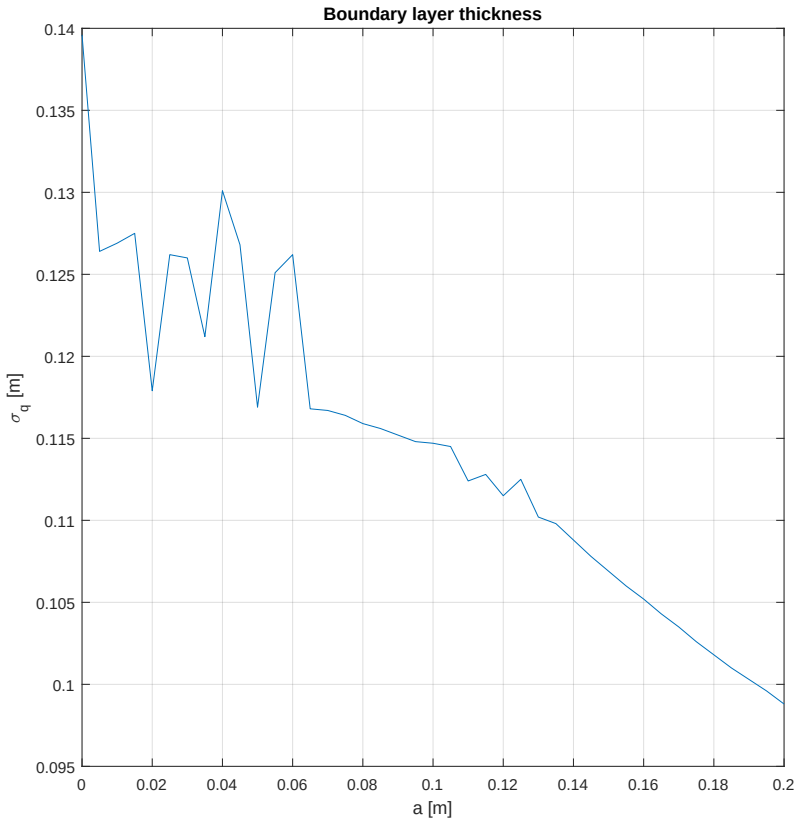

Figure 5.3. Dependency of the boundary layer thickness for the standard deviation for the edgewise tip displacement σ_q, $\tau_0 = 100$, $\mu_0 = 0.1$, $\tau_1 = \tau_2 = \tau_3 = \tau_4 = \mu_1 = \mu_2 = \mu_3 = \mu_4 = 0$

As can be seen in figure 5.3, the boundary layer thickness causes some variation in the standard deviation for the edgewise tip displacement, until it reaches a certain point. The rapid variation at small values of a is believed to be due to numerical estimation errors. It seems with bigger boundary layers a greater damping effect is achieved, which would suggest the maximum available space should be used for the boundary layer. Obviously, the diameter of the cross-section of the torus must be smaller than the height of the cross section of the blade h_1. Hence the maximum value of the boundary layer $a < \frac{h_1}{2}$. Because this is tested for a specific set of values for the parameters of τ_y and μ, in order to verify, that this also works for the semi-active control that is being investigated, this is tested for model B seen in chapter 4 equation 4.23. The result can be seen in figure 5.4.

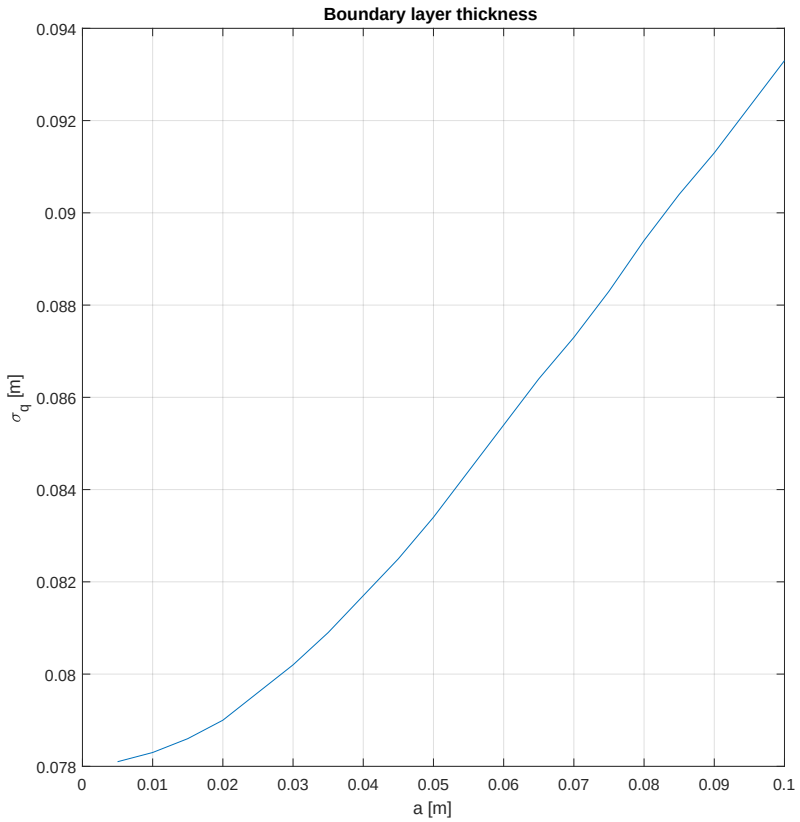

Figure 5.4. Dependency of the boundary layer thickness for the standard deviation for the edgewise tip displacement σ_q, for model B parameters in Equation 4.23.

As seen in figure 5.4 the change in boundary layer thickness makes causes an increase of the standard deviation for the edgewise tip displacement, which would suggest that in the damping model that c_1 and c_2 can be changed depending on what is available. This would mean that, for the optimized situation can be a variation of $\mu(t), \tau_y(t)$ and a. This means that the boundary layer thickness can be one of the tuning parameters with $\overline{\tau}$ and $\overline{\mu}$. This can not be generalized, as it is only for certain for this model. Therefore this statement can only account for the model that is being worked with in this project. But it does give more options when trying to control the standard variation σ_q.

5.1.2 Rotational speed

Looking at the equation of motion for the reduced 2-DOF in 2.21 and 2.22 it can be seen that Ω is present in many parts of the system, so something is bound to change and be optimized differently for different rotational speed. Up until now the value of $\Omega = 1.267\,\text{rad/s}$, in this parameter variation the values of Ω is chosen to be:

$$\Omega_1 = 0.4223\,\text{rad/s}, \qquad \Omega_2 = 0.8447\,\text{rad/s} \tag{5.1}$$

The values in equation 5.1 corresponds to $\frac{1}{3}$ and $\frac{2}{3}$ of the starting value.
The smart fluid model, the values in equation 5.1 is used for Model B in equation 4.23. The results for varying the values of Ω is:

$$\begin{aligned} &\Omega_1 = 0.4223\,\text{rad/s} \;\Rightarrow\; \sigma_{q,smart} = 0.1040\,\text{m} \\ &\Omega_2 = 0.8447\,\text{rad/s} \;\Rightarrow\; \sigma_{q,smart} = 0.0800\,\text{m} \end{aligned} \tag{5.2}$$

From the results it can be seen that for slower rotational speeds would yield larger excitations which means that the model is poorly optimized for this specific scenario. In contrast, the semi-active control with smart fluids offers an option for instantaneous change of the tuning of the damper to the changed rotational speed. By doing this the analysis made in chapter 4 could be done all over again to then find the new optimized values.

Model for Ω_1 :

$$\overline{\tau} = \begin{bmatrix} \tau_0 \\ \tau_1 \end{bmatrix} = \begin{bmatrix} 25000 \\ 14000 \end{bmatrix} \frac{N}{m^2}, \quad \overline{\mu} = \begin{bmatrix} \mu_0 \\ \mu_1 \end{bmatrix} = \begin{bmatrix} 50 \\ 83 \end{bmatrix} \frac{Ns}{m^2}, \quad \sigma_q = 0.0984\,\text{m} \tag{5.3}$$

Model for Ω_2 :

$$\overline{\tau} = \begin{bmatrix} \tau_0 \\ \tau_1 \end{bmatrix} = \begin{bmatrix} 8000 \\ 5700 \end{bmatrix} \frac{N}{m^2}, \quad \overline{\mu} = \begin{bmatrix} \mu_0 \\ \mu_1 \end{bmatrix} = \begin{bmatrix} 15 \\ 125 \end{bmatrix} \frac{Ns}{m^2}, \quad \sigma_q = 0.0795\,\text{m} \tag{5.4}$$

From the equation 5.3 and 5.4 it can be seen the values of the vectors $\overline{\tau}$ and $\overline{\mu}$ suggests different values depending on the rotational speeds, which is where the smart liquids can adapt via the semi-active control. Therefore the semi-active control can be beneficial where the passive control do not contribute with enough damping for the system.
In Chapter 4 the conclussion was that a semi-active control law is to be dependent on the rotational speed of the rotor, therefore an analysis is made with the same values as for the smart fluid seen in Equation 5.1 to see if the optimal ξ changes with the rotational velocity as anticipated.
With the optimized passive value for $\xi = 5.68$, the standard deviation σ_q for the two rotor

velocities is:

$$\begin{aligned} \Omega_1 = 0.4223\,\text{rad/s} \;&\Rightarrow\; \sigma_{q,orifice} = 0.1076\,\text{m} \\ \Omega_2 = 0.8447\,\text{rad/s} \;&\Rightarrow\; \sigma_{q,orifice} = 0.0816\,\text{m} \end{aligned} \tag{5.5}$$

From Equation 5.5 the passive control do not seem to be best choice any more, which is where the semi-active control comes to it rights. By setting $\xi_1 = 200$ in Equation 4.7 the standard deviation will be reduced to $\sigma_{q,orifice} = 0.0791\,\text{m}$ for rotational speed $\Omega_2 = 0.8447\,\text{rad/s}$. For $\Omega_1 = 0.4223\,\text{rad/s}$ the value of $\xi_1 = 500$ the standard deviation is $\sigma_{q,orifice} = 0.1047\,\text{m}$.
These values for ξ_1 can of course be found by optimization, but because of time limited, a few values was quickly found to show that the standard deviation can be lowered from the optimized passive control when looking at varying rotational speed for the rotor.

5.2 Practical Implications

On a practical approach to the problem, the semi-active control can be difficult to establish. The different solutions each has different problems. Looking at the orifice control, some mechanism that should fit into the wind turbine wing with the torus containing the liquid, in this case just water, could prove difficult to fit in the very limited space that is available.
A solution powered by electricity to control the orifice opening could be possibly be implemented but then response time of this system could prove to be an issue since more connections is in place but not enough time to make the change happen before the next adaptation is needed.

For the smart liquid solution, the difficulty lies else where, because not many adjustments is required to the torus to enabling it to create a magnetic field see Figure 3.3. The issue comes with the liquid itself, the dwelling of the magnetic particles in the should not be an issue even though the wind turbine wing do not move for quite some time when it is transported from the factory to the assembly point, but because of the quick motion when it is active the magnetic particles in the smart liquid would be stirred up again.
The difference when looking at water as a damping liquid and smart liquid is in the weight of the liquid. As mentioned earlier the smart liquid weighs approximately three times as much which could cause issues when implemented, not to mention it is difficult to acquire as it is a relatively new product and few manufactures, which possibly also means it is expensive as well in the needed quantities.

Conclusion 6

Two different methods is proposed for the semi-active control of the damping mechanism for the edgewise tip displacement for the wind turbine blade. The orifice control with basis in control the relative opening of the orifice in order to change the inertia force which counter act the excitation, did not have the sufficient capabilities in order to dampen the motion any better than the optimized passive controller. It showed the acceleration of the fluids motion inside damper was being reduced with the relative opening closing, which should have been the opposite, with a greater acceleration. The smart fluid control is to use a magnetic field to alter the characteristics of the fluid in order to achieve optimized damping capabilities, which for the specific rotational speed the result of it being an alternative to the passive controller since the standard deviation of the edgewise tip displacement is 0.4% different.

The rotational speed was changed in order to see how it would change the system and the impact it would have on the parameters for the orifice control and the smart fluid control. It caused some changes, which increased the standard deviation as expected, since the damper is not optimized for the new rotational speeds tested. In order to keep the standard deviation down, the values in the model is changed to lower the standard deviation, to find a more optimized solution for the specific rotational speed. A lower standard deviation σ_q was obtained for the different rotational velocities, which suggest that the semi-active control can work as long as the response time for the change is instantaneous. Therefore the smart liquid is a good solution as the magnetic field which controls the liquid has instantaneous response time.

For practical purpose the semi-active control can be difficult to implement in the wind turbine wing, because for the orifice control, a mechanism to control the opening is required and it should also have instantaneous response time, which is difficult to make, as there is already limited space at the dampers position in the wing to install anything that ensures that.

The smart liquid solution can work, but as mentioned earlier the difficulty is in the mass of liquid and the acquisition of the smart liquid. As for one wind turbine, three dampers is needed which is going to be expensive as it is a relatively new technology which is not widely used yet or easily made.

Overall semi-active control of smart liquids is a viable alternative as a damping mechanism.

Bibliography

Basu et al., **2015**. Zhang Basu et al., Nielsen. *Damping of edgewise vibration in wind turbine blades by means of circular liquid dampers*. Wiley Online Library, -, 213–226, 2015.

Goncalves, **2005**. Fernando D. Goncalves. *Characterizing the Behavior of Magnetorheological Fluids at High Velocities and High Shear Rates*. Virginia Polytechnic Institute and State University, -, 1–103, 2005.

Jiles, **1998**. David C. Jiles. *Introduction to Magnetism and Magnetic Materials, Secound Edition*. ISBN: 978-0-412-79860-3, -. 1998.

J.Y. Wang, **2005**. J.M. Ko B.F. Spence Jr. J.Y. Wang, Y.Q. Ni. *Magneto-rheological tuned liquid column dampers (MR-TLCDs) for vibraiton mitigation of tall buildings: modelling and analysis of open-loop control*. ELSEVIER, -, 2023–2034, 2005.

J.Y. Wang, **2004**. J.M. Ko B.F. Spence Jr. J.Y. Wang, Y.Q. Ni. *Stochastic optimal control of wind-excited tall buildings using semi-active MR-TLCDS*. ELSEVIER, -, 269–277, 2004.

Lord Corporation, **2011**. Lord Corporation. *MRF-132DG Magneto-Rheological Fluid*, 2011. Technical data for MR-fluid MRF-132DG.

Mark R. Jolly, **2000**. J. David Carlson Mark R. Jolly, Jonathan W. Bender. *Properties and Applications of Commercial Magnetorheological Fluids*. Journal of Intelligent Material Systems and Structures, -, 5–13, 2000.

Michael D. Symans, **1997**. Michael C. Constantinou Michael D. Symans. *Semi-active control systems for seismic protection of structures: a state-of-the-art review*. ELSEVIER, -, 469–487, 1997.

N.R. Fisco, **2011**. H. Adeli N.R. Fisco. *Smart structures: Part I - Active and semi-active control*. Scientia Iranica, Sharif University of Technology, -, 275–284, 2011.

Reece, **2006**. Peter L. Reece. *Smart Materials and Structures*. ISBN: 978-1-61668-118-0, -. Nova Science Publishers, Inc, 2006.

Wikipedia, **2017**. Wikipedia. *Magnetorheological fluid*. URL: `https://en.wikipedia.org/wiki/Magnetorheological_fluid`, 2017. Figures used from the article, downloaded 09-03-2017.